Optimized Differential GFSK Demodulator

Bo Yu, *Student Member, IEEE*, Liuqing Yang, *Senior Member, IEEE*, and Chia-Chin Chong, *Senior Member, IEEE*

***Abstract*—Gaussian frequency shift keying (GFSK) is a promising digital modulation scheme. The design of simple and high-performance receivers for GFSK systems is a challenging task. In this letter, we develop an optimized differential GFSK demodulator and investigate the phase wrapping issue in its implementation. Simulation results show bit-error-rate (BER) performance improvement in comparison with conventional differential demodulators in both AWGN and flat fading channels. We also compare our proposed demodulator with other existing alternatives in terms of BER performance.**

***Index Terms*—Gaussian frequency shift keying (GFSK), differential demodulation, phase wrapping.**

I. Introduction

GAUSSIAN Frequency Shift Keying (GFSK) is an important digital modulation scheme. It is widely used in low cost and low power consumption systems such as Bluetooth in the unlicensed 2.4 GHz industrial, scientific and medical (ISM) band due to its spectral efficiency, constant signal envelope property and the possibility for low complexity receivers.

The optimum GFSK receiver consists of a correlator followed by a maximum-likelihood sequence detector that searches for the minimum Euclidean distance path through the state trellis based on Viterbi algorithm [1], [2]. However, due to the complexity of the matched filter bank and carrier synchronization, such a receiver has very limited applications. In addition, these designs always assume a certain nominal value for the modulation index h. However, the modulation index may vary in a relatively wide range (for Bluetooth, the modulation index is allowed to vary between 0.28 and 0.35), leading to a varying trellis structure for sequence detection with possibly tremendous number of states. All these render this optimum receiver impractical. Hence noncoherent suboptimal receivers are typically preferred, especially in systems where it is desirable to have a simpler receiver structure.

A simple limiter-discriminator followed by integrate-and-dump post-detection filtering [1], [3] is often employed to demodulate GFSK signals. The resulting receiver is called limiter-discriminator with integrator (LDI) receiver. The LDI receiver is low-cost and easy to implement, but it suffers from a relatively poor power efficiency compared to more sophisticated receivers. Another simple noncoherent receiver is the phase differential detector [3], [4]. These receivers are also applicable to a relatively large range of modulation indices.

There are also some other schemes in literature. In [5], Lee proposed a zero-intermediate frequency zero-crossing demodulator (ZIFZCD). The performance of this demodulator is not as good as the LDI detector. Later, Scholand and Jung proposed another demodulator [6] based on zero-crossing detection of the a real-valued received signal at an appropriately chosen intermediate frequency (IF) in combination with a decorrelating matched filter. The receiver performance has some improvements compared to the conventional baseband zero-crossing detectors and has similar performance as the baseband differential detector and the LDI detector. More recently, Lampe *et.al.* proposed a noncoherent sequence detector [7] based on Rimoldi's decomposition of the GFSK transmit signal. This receiver can achieve significant performance gain of more than 4 dB over the discriminator-based detector. The main disadvantage is the complexity required for a two-state trellis search. In their subsequent paper [8], Ibrahim *et.al.* considered sequence detection based on Laurent's decomposition of the GFSK transmit signal. The result shows a performance close to the limit of maximum-likelihood sequence detection. However, this receiver still requires the modulation index to be known at the receiver. When the modulation index is not available, it has to go through an adaptation period to search for the modulation index.

In this letter, we develop a simple demodulator for GFSK receivers, which averages the phase based on the signal-to-noise ratio (SNR) maximizing criterion, and does not require knowledge of the exact modulation index. Compared to demodulators with similar complexity, such as the LDI, our proposed receiver can achieve superior performance. The paper is organized as follows. In Section II, we will briefly introduce the GFSK transmission model. Then we will propose an optimized differential demodulator in Section III. The receiver performance is studied in Section IV, followed by summarizing remarks in Section V.

II. GFSK Transmission Model

In this section, we will briefly describe the GFSK transmission model.

A. GFSK signal model

A passband transmitted GFSK signal can be represented as [4]

$$s(t,\boldsymbol{\alpha}) = \sqrt{\frac{2E_b}{T}}\cos[2\pi f_0 t + \varphi(t,\boldsymbol{\alpha}) + \varphi_0], \qquad (1)$$

Paper approved by E. Perrins, the Editor for Modulation Theory of the IEEE Communications Society. Manuscript received January 12, 2010; revised September 22, 2010 and January 14, 2011.

This work was supported by DOCOMO USA Labs. Parts of the results in this paper have been presented at the 43rd Asilomar Conference on Signals, Systems and Computers, Pacific Grove, CA, November 2009.

B. Yu and L. Yang are with the Department of Electrical and Computer Engineering, Colorado State University, 1373 Campus Delivery, Fort Collins, CO 80523-1373, USA (e-mail: boyu@lamar.colostate.edu, lqyang@engr.colostate.edu).

C.-C. Chong is with DOCOMO USA Labs, 3240 Hillview Avenue, Palo Alto, CA 94304 (e-mail: cchong@docomolabs-usa.com).

Digital Object Identifier 10.1109/TCOMM.2011.041111.100010A

where E_b is the energy per bit, T is the symbol period, f_0 is the carrier frequency, φ_0 is an arbitrary constant phase shift. The output phase deviation $\varphi(t,\boldsymbol{\alpha})$ is determined by the input data sequence $\boldsymbol{\alpha} = ..., \alpha_{-2}, \alpha_{-1}, \alpha_0, \alpha_1, \alpha_2, ...$ with $\alpha_i \in \{\pm 1\}$:

$$\varphi(t,\boldsymbol{\alpha}) = 2\pi h \sum_{i=n-L+1}^{n} \alpha_i q(t-iT) + \pi h \sum_{i=-\infty}^{n-L} \alpha_i \,, \quad (2)$$

where h is the modulation index, $q(t) = \int_{-\infty}^{t} g(\tau)d\tau$ with

$$g(t) = Q\left(\gamma \cdot BT\left(\frac{t}{T} - \frac{1}{2}\right)\right) - Q\left(\gamma \cdot BT\left(\frac{t}{T} + \frac{1}{2}\right)\right),$$

being the frequency pulse with constant $\gamma = 2\pi/\sqrt{\ln 2}$ and $Q(\cdot)$ is the Gaussian Q-function. BT is the 3 dB bandwidth-time product. Generally speaking, the smaller the BT values, the more significant the ISI introduced due to the increase of the effective frequency pulse duration. In the Bluetooth standard [9], h can vary between 0.28 and 0.35 and BT equals 0.5 with $T = 10^{-6}$s, giving rise to a $g(t)$ with effective duration of $2T$.

B. Baseband equivalent system model

The channel model considered is Rayleigh flat fading with additive white Gaussian noise (AWGN).

The received signal is first passed through a receiver filter with transfer function $H_r(f)$, then the phase differential detection is performed on the output signal of the filter. The input signal to the receiver filter is

$$\tilde{r}(t) = e^{j\theta(t)} h(t) * s_l(t) + n(t), \quad (3)$$

where $\theta(t)$ is the time-varying channel phase, $h(t)$ is the channel impulse response represented by a single discrete-time complex filter tap $h_0 \sim \mathcal{CN}(0,1)$, $n(t)$ is zero mean white Gaussian noise with single-sided spectral density N_0, and $s_l(t)$ is the complex envelope of the GFSK transmitted signal

$$s_l(t) = \rho \exp[j(\varphi(t,\boldsymbol{\alpha}) + \varphi_0)]. \quad (4)$$

We assume that the receiver filter has sufficient bandwidth such that it will introduce negligible distortion on the signal while bandlimiting the noise. Thus the output of the receiver filter is

$$r(t) = e^{j\theta(t)} h(t) * s_l(t) + \eta(t), \quad (5)$$

where $\eta(t) = \eta_r(t) + j\eta_i(t)$ is bandlimited zero mean Gaussian noise with autocorrelation

$$R_\eta(\tau) = N_0 \int_{-\infty}^{\infty} |H_r(f)|^2 \exp(j2\pi f\tau) df, \quad (6)$$

and average power

$$P_\eta = R_\eta(0) = N_0 \int_{-\infty}^{\infty} |H_r(f)|^2 df \triangleq N_0 B_n, \quad (7)$$

where B_n is the equivalent noise bandwidth of the receiver filter. We assume that $\theta(t)$ does not change over a symbol period. For the phase differential demodulation, we take the difference of consecutive phase samples, the unknown phase is thus canceled. In addition, η_r and η_i are independent and each has a distribution of $\mathcal{N}(0,\sigma^2)$, where the variance σ^2 is defined as $\sigma^2 = R_\eta(0) = N_0 B_n$. Hence the joint distribution of η_r and η_i is

$$f_{\eta_r\eta_i}(x,y) = \frac{1}{2\pi\sigma^2} e^{-\frac{x^2+y^2}{2\sigma^2}}. \quad (8)$$

III. Optimized GFSK Demodulator

In this section, we first present the basic ideas of conventional phase differential demodulation. To facilitate the design of our optimized differential demodulator, the phase noise distribution is then derived. Based on the phase noise distribution, we will then propose an optimized differential demodulator and investigate the phase wrapping problem.

A. Differential GFSK Demodulation

In this subsection, we consider the basic ideas about differential demodulation in AWGN. For Bluetooth standard, the effective frequency pulse duration is $2T$, giving rise to a piecewise monotonic phase trellis within each symbol duration. The direction of the monotonic change is determined by the binary symbol value. Hence, a phase differential demodulator can be employed. We first extract the phase of the received signal

$$\phi(t) = \sphericalangle r(t) = \varphi(t) + \phi_\eta(t), \quad (9)$$

where $\varphi(t)$ is determined by the transmitted phase and $\phi_\eta(t)$ is a random variable due to the AWGN. Essentially, the conventional differential demodulator involves sampling $\phi(t)$ in (9) at symbol rate to obtain $\phi(nT)$ and then taking the difference of the neighboring samples

$$\Delta\phi(nT) = \phi(nT) - \phi(nT - T).$$

A decision can then be made based on the sign of $\Delta\phi(nT)$. However, due to the randomness of the phase noise, the decision based on a single phase sample per symbol lacks sufficient reliability so that conventional differential demodulator suffers from degraded performance.

Intuitively, one can average a portion of every symbol-long trellis segment instead of a single sample at each end before taking the difference. This may provide some gain in the signal-to-noise ratio (SNR). In the case of Gaussian noise, the gain in SNR leads to improvement in BER. To facilitate the design of an optimum differential demodulator, we will next study the distribution of phase noise $\phi_\eta(t)$. For the simplification of analysis, we will first consider the AWGN channel. The result can then be easily extended to flat fading channels.

B. Phase Noise Distribution

For notational simplicity, let $\varphi(t) = 0$ in (9) without loss of generality. It then follows that $\phi(t) = \phi_\eta(t)$. Denote the probability density function (PDF) and the cumulative density function (CDF) of the random variable $\phi(t)$ as $f_\phi(\varphi)$ and $F_\phi(\varphi)$, respectively. We first consider $0 \le \phi(t) \le \pi/2$, on which

$$\begin{aligned} F_\phi(\varphi) &= Pr(0 \le \phi \le \varphi) \\ &= \int_{-\rho}^{\infty} \int_{0}^{(\rho+x)\tan\varphi} f_{\eta_r\eta_i}(x,y)\, dy\, dx. \end{aligned} \quad (10)$$

Then by Leibnitz's rule, the PDF is derived as

$$\begin{aligned} f_\phi(\varphi) &= \frac{d}{d\varphi}F_\phi(\varphi) \\ &= \frac{1}{2\pi\sigma^2}\int_{-\rho}^{\infty} e^{-\frac{x^2+(\rho+x)^2\tan^2\varphi}{2\sigma^2}}\frac{d}{d\varphi}[(\rho+x)\tan\varphi]\,dx \\ &= \frac{1}{2\pi}e^{-\frac{\rho^2}{2\sigma^2}} + \frac{\rho\cos\varphi}{\sqrt{2\pi}\sigma}e^{-\frac{\rho^2\sin^2\varphi}{2\sigma^2}}Q\left(-\frac{\rho\cos\varphi}{\sigma}\right). \end{aligned} \tag{11}$$

For $\pi/2 < \phi(t) < 2\pi$, only the integral interval in (10) is slightly different for each quadrant, and it can be readily shown that the final PDF results are the same as (11) for all $\phi(t)$ values.

At high SNR (large ρ), we have $\exp(-\frac{\rho^2}{2\sigma^2}) \approx 0$ and $Q(-\frac{\rho\cos\phi}{\sigma}) \approx 1$. As a result, the complicated noise distribution can be approximated as:

$$f_\phi(\varphi) \approx \frac{1}{\sqrt{2\pi}\sigma/\rho}\cdot e^{-\frac{1}{2}\cdot\frac{\varphi^2}{(\sigma/\rho)^2}}, \tag{12}$$

which is simply the Gaussian distribution with zero mean and variance $(\sigma/\rho)^2$. Such a Gaussian approximation of the phase noise distribution can be very useful if the approximation is accurate. This is because our demodulator design is intended to optimize the ultimate BER performance of the system. In the case of Gaussian noise, minimizing BER is equivalent to maximizing the SNR, leading to a readily-achievable SNR-maximizing system optimization criterion. This is generally not true for non-Gaussian noise [10].

In order to assess the accuracy of our approximation, we perform two sets of simulations. In the first simulation, we compare the true and approximate PDF curves at various SNR values. As shown in Fig. 1, we observe that these curves are already very close at $\rho^2/(2\sigma^2) = 2$ dB, and are nearly identical at $\rho^2/(2\sigma^2) = 8$ dB. We also simulate and compare the BER performance of a simple binary system where the additive noise follows either the true noise PDF or the Gaussian approximation. The result in Fig. 2 shows that the BER performances of the two are very similar. You may note that the BER gap at higher SNR seems to be larger than the gap at lower SNR. However, since the scale is different in the BER axis, the approximation is actually much better at higher SNR, which confirms our previous analysis.

So far, we have verified that the noise in the extracted phase can be well approximated as Gaussian distributed. With all the knowledge above, we will develop our optimized differential GFSK demodulator in the following subsection.

C. Optimized Differential GFSK Demodulator

Each symbol-long phase trellis segment can take one of the four shapes depending on the specific symbol sequence. For example, for an input data sequence of $(1,-1,1,-1,1,1,1,1)$, the phase trellis during $[0,T)$ is linear in the first half and nonlinear in the second half (which we term as type D); the phase trellis during $[T,2T)$ is nonlinear throughout the entire duration (which we term as type C); the phase trellis during $[4T,5T)$ is nonlinear in the first half and linear in the second half (which we term as type B); and the phase trellis during $[5T,6T)$ is linear throughout (which we term as type A). Without loss of generality, we will start from the linear phase segment and then generalize to the nonlinear and partly nonlinear ones.

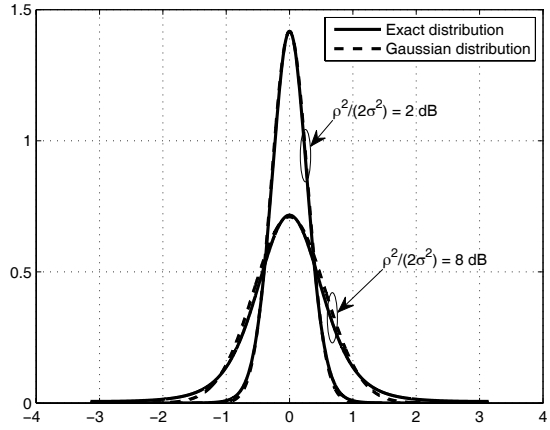

Fig. 1. PDF curves for $\rho^2/(2\sigma^2) = 2$ dB and $\rho^2/(2\sigma^2) = 8$ dB.

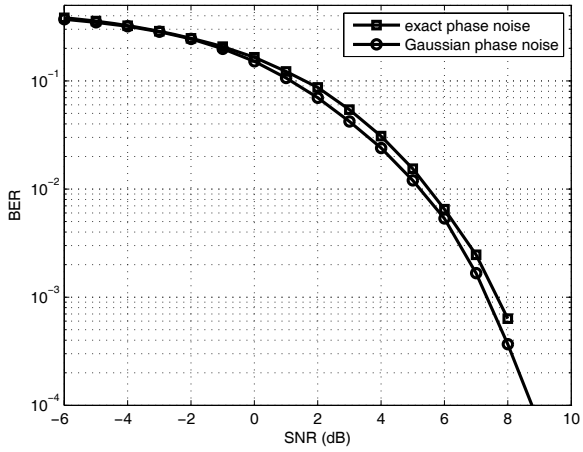

Fig. 2. BER performance for the exact phase noise and the approximated Gaussian phase noise.

A linear phase curve segment has a function $q(t) = A\cdot t/T$, $t \in [0,T)$. Note that the scalar A is proportional to the modulation index h. However, since its value does not affect the optimization result, we will normalize it to 1 for notational simplicity (the same for the nonlinear phase curve cases). Let T_o be the portion at each end of this segment over which we average before taking the difference, as illustrated in Fig. 3. Then the resultant SNR is:

$$\mathrm{SNR}_A(T_o) = \frac{\left(\int_{T-T_o}^{T}\frac{t}{T}dt - \int_0^{T_o}\frac{t}{T}dt\right)^2}{2T_o\sigma^2}. \tag{13}$$

As we have shown in the preceding subsection, the phase noise can be well approximated as Gaussian distributed even at fairly low SNR. Hence, the SNR-maximizing T_o is essentially also BER-minimizing. Maximizing SNR_A for a given symbol duration T and A^2/σ^2, we obtain

$$\max_{0\le T_o\le T/2}\mathrm{SNR}_A(T_o) = \max_{0\le T_o\le T/2}\frac{T_o(T-T_o)^2}{2T^2\sigma^2}, \tag{14}$$

which results in $T_o = T/3$. This indicates that one should average the first and last 33% of each symbol-long phase

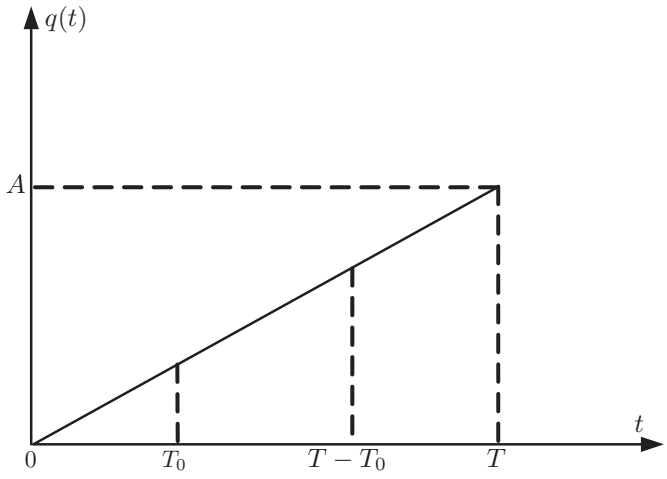

Fig. 3. Linear phase curve model.

segment and then take their difference on which a decision can be made.

Next we consider the type-C phase segment during $[T, 2T)$. The exact function for this segment does not have a closed form (containing the integral of Gaussian Q function). However we notice that each half of the segment curves in the shape of parabola approximately. Hence we use two second-order polynomials to fit each half; that is $x_1(t) = -0.9202(t/T)^2 - 0.1797(t/T) + 0.8158$, $t \in [0, 0.5T)$, and $x_2(t) = 0.9202(t/T)^2 - 1.9911(t/T) + 1.273$, $t \in [0.5T, T)$. Accordingly, the resultant SNR after averaging and difference taking is:

$$\mathrm{SNR}_C(T_o) = \frac{\left(\int_{T-T_o}^{T} x_2(t)dt - \int_0^{T_o} x_1(t)dt\right)^2}{2T_o\sigma^2}. \tag{15}$$

As a result, the optimal portion should be chosen as $T_o = 0.3675T$.

Similar results can be obtained for type-B and type-D phase segments. Due to the space limit, these are omitted here. Since the four different shapes occur with equal probability, one can also find the overall optimum T_o by solving

$$\max_{0\le T_o\le T/2}[\mathrm{SNR}_A(T_o) + \mathrm{SNR}_B(T_o) + \mathrm{SNR}_C(T_o) + \mathrm{SNR}_D(T_o)], \tag{16}$$

which results in $T_o = 0.35T$.

The continuous-time analysis can be readily extended to the discrete-time sampled phase segments. Let $2K$ denote the number of samples per symbol. The problem now is to determine the optimum M, which is the number of samples to be averaged at each end of the $2K$ samples per symbol. Denote the second group of M samples as $S_1, ..., S_M$, and the first group of M samples as $S'_1, ..., S'_M$. It then follows that $S_i = (K-1+i)/(2K-1) + \eta_i$ and $S'_i = (i-1)/(2K-1) + \eta'_i$, $i = 1, \ldots, M$. Consider again the type-A linear phase segment. With the Gaussian approximation of the phase noise, the difference between the two averages is $\sum_{i=1}^{M}(S_i - S'_i)/M$, leading to an SNR of

$$\mathrm{SNR}_A^{(d)}(M) = \frac{M(2K-M)^2}{2(2K-1)^2\sigma^2}, \tag{17}$$

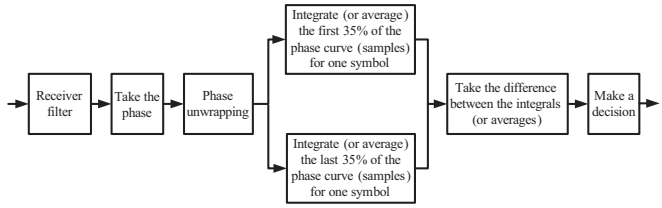

Fig. 4. Block diagram of our optimized differential demodulator.

where superscript (d) indicates discrete-time. Clearly, $\mathrm{SNR}_A^{(d)}(M)$ bears a form very similar to $\mathrm{SNR}_A(T_o)$ in (13). Not surprisingly, maximizing $\mathrm{SNR}_A^{(d)}(M)$ results in $M = 2K/3$, which agrees perfectly with the continuous-time result. Using the same methodology, we can obtain the optimum M for the general case as $M = 0.7K$. Thus, by choosing the optimal M, the SNR is maximized and the error probability minimized.

The block diagram of our optimized differential demodulator is shown in Fig. 4. We can see that the only difference between this new demodulator and the conventional differential one is the averaging part. To evaluate the performance gain by using the optimized differential demodulator, we notice that the conventional differential demodulator can be considered as a special case with $M = 1$ for any K values. Considering again the type-A phase segment, and evaluating (17) at $M = 2K/3$ and $M = 1$ and taking the relative ratio, we obtain the SNR gain over conventional differential demodulator as:

$$\frac{\mathrm{SNR}_A^{(d)}(2K/3)}{\mathrm{SNR}_A^{(d)}(1)} = \frac{32}{27}\frac{K^3}{(2K-1)^2}. \tag{18}$$

This gain is a function of K because the optimum number of averaged samples M is dependent on the total number of available samples $2K$. The above results can be readily extended to the flat fading channels since each realization of the channel fading coefficient is essentially an AWGN case. All these results will be verified by simulations.

D. Phase Wrapping Problem

When realizing these phase differential demodulation algorithms, however, there is an implementation problem. Recall that our differential operations are performed on the phase function $\phi(t)$ in (9). Unlike the original phase trellis $\varphi(t, \boldsymbol{\alpha})$ in (2), $\phi(t)$ is not only noisy, but also suffers from the phase wrapping problem since it assumes a finite range of 2π.

To solve this problem, conventional differential demodulator in [4] takes the following structure: the received signal $r(t)$ is multiplied by a T-delayed and $\pi/2$ phase-shifted version of itself and then sampled at the symbol rate to give the decision statistic. These operations will essentially give $\sin[\Delta\phi(nT)]$ without explicitly extracting $\phi(t)$, thus avoiding the phase wrapping problem. Since the decision only relies on the sign of $\Delta\phi(nT)$, the above operations leading to $\sin[\Delta\phi(nT)]$ generally preserves this sign information. However, for large modulation index $h \ge 1$, the phase change $\Delta\phi(nT)$ over one symbol duration may exceed π. In this case, the $\sin$ operator cannot preserve the sign of $\Delta\phi(nT)$ anymore.

Hence, in both the conventional and optimized differential demodulators, we directly deal with the phase extracted from

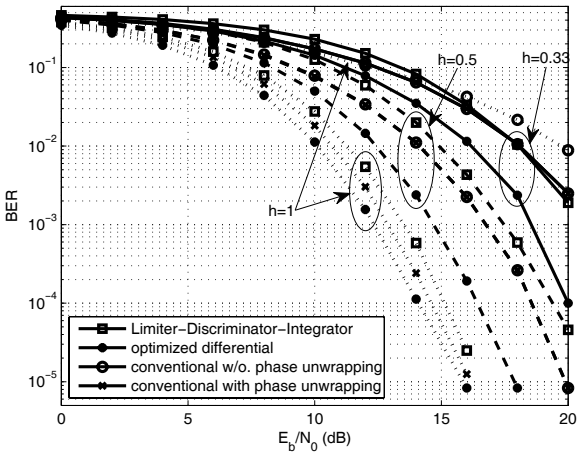

Fig. 5. BER performance in AWGN channels.

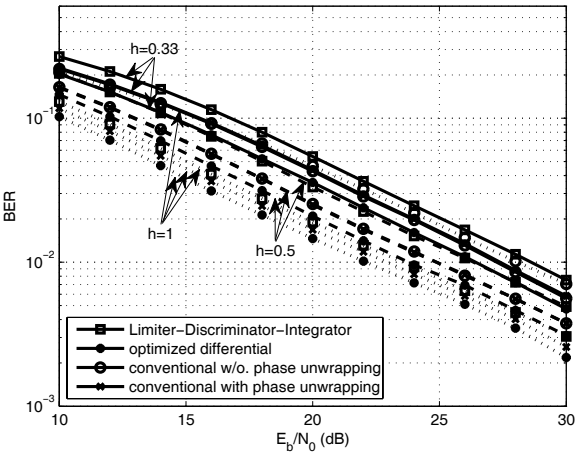

Fig. 6. BER performance in flat fading channels.

the received signal. Specifically, the phase is unwrapped by simply adding $\pm 2\pi$ when the absolute change between the consecutive phase samples are greater than the jump tolerance π. Both methods are tested and compared by simulations in the next section.

IV. Performance Evaluation and Discussion

In this section, we will evaluate the performance of our proposed demodulator by simulations in terms of BER versus E_b/N_0, where E_b is the signal energy per information bit and N_0 is the power spectral density of the additive noise. In all simulations, we set $BT = 0.5, B_nT = 1$ and take 8 samples per symbol.

Figs. 5 and 6 show the BER performance of our optimized differential demodulator together with that of the conventional one and the LDI demodulator with different modulation indices h in AWGN and flat fading channels, respectively. In particular, for the conventional differential demodulator, we simulated both the system in [4] which avoids phase wrapping as well as our direct unwrapping approach. We observe that, the optimized demodulator shows about 1$\sim$2 dB improvement over the conventional differential receivers and the LDI especially at high SNR. Note that, for small h ($h = 0.33$ or 0.5), phase unwrapping does not lead to any performance improvement in the conventional receiver. This confirms that the performance gain is entirely due to our optimized demodulation algorithm. This result is also consistent with the theoretical result obtained in (18) with $K = 4$. Note that the complexity of LDI is similar to the optimized demodulator since LDI also needs oversampling.

In addition, in both cases, as h increases, the performances of all demodulators except the conventional scheme without phase unwrapping in [4] improve accordingly. We note that when $h = 1$, the conventional differential demodulator in [4] suffers from significant performance loss. This is because the phase change during one symbol interval may exceed π for large h ($h = 1$) such that the sin operator cannot preserve the sign of $\Delta\phi(nT)$ anymore. In addition, the gain of the optimized demodulator over the conventional one for large h is not as significant as that for small h. This is due to the phase unwrapping operation. As h increases, the phase change over one symbol interval will increase. However, the error introduced to the recovered phase by phase unwrapping operation will also increase. Therefore the BER performance improvement is not a strictly increasing function of the modulation index h.

V. Conclusions

In this letter, we have developed an optimized phase differential demodulator for GFSK modulated systems including Bluetooth. Performance of this demodulator has been studied by theoretical analysis and simulations. It has been shown that the optimized demodulator can achieve evident improvements over the conventional demodulators and provide a favorable performance in both AWGN and flat fading channels.

References

[1] A. Soltanian and R. E. V. Dyck, "Performance of the Bluetooth system in fading dispersive channels and interference," in *Proc. IEEE Global Telecommun. Conf.*, vol. 6, Nov. 2001, pp. 3499-3503.

[2] W. Jia, A. Nallanathan, and H. K. Garg, "Performance of a Bluetooth system in multipath fading channels and interference," in *Proc. IEEE Workshop Mobile Wireless Commun. Netw.*, Sep. 2002, pp. 579-582.

[3] M. K. Simon and C. C. Wang, "Differential versus limiter-discriminator detection of narrow-band FM," *IEEE Trans. Commun.*, vol. 31, no. 11, pp. 1227-1234, Nov. 1983.

[4] J. B. Anderson, T. Aulin, and C.-E. Sundberg, *Digital Phase Modulation*, 1st edition. Springer, 1986.

[5] E. K. B. Lee, "Zero-crossing baseband demodulator," in *Proc. IEEE International Symp. Personal, Indoor Mobile Radio Commun.*, vol. 2, Sep. 1995, pp. 466-470.

[6] T. Scholand and P. Jung, "Novel receiver structure for Bluetooth based on modified zero-crossing demodulation," in *Proc. IEEE Global Telecommun. Conf.*, vol. 2, Dec. 2003, pp. 729-733.

[7] L. Lampe, R. Schober, and M. Jain, "Noncoherent sequence detection receiver for Bluetooth systems," *IEEE J. Sel. Areas Commun.*, vol. 23, no. 9, pp. 1718-1727, Sep. 2005.

[8] N. Ibrahim, L. Lampe, and R. Schober, "Bluetooth receiver design based on Laurent's decomposition," *IEEE Trans. Veh. Technol.*, vol. 56, no. 4, pp. 1856-1862, July 2007.

[9] Bluetooth Special Interest Group (SIG). Available: http://www.bluetooth.org

[10] B. V. K. V. Kumar, A. Mahalanobis, and R. D. Juday, *Correlation Pattern Recognition*. Cambridge University Press, 2005.